Mutations in *TRAPPC12* Manifest in Progressive Childhood Encephalopathy and Golgi Dysfunction

Miroslav P. Milev,[1] Megan E. Grout,[2] Djenann Saint-Dic,[1] Yong-Han Hank Cheng,[2] Ian A. Glass,[2] Christopher J. Hale,[3] David S. Hanna,[3] Michael O. Dorschner,[3] Keshika Prematilake,[1] Avraham Shaag,[4] Orly Elpeleg,[4] Michael Sacher,[1,6,*] Dan Doherty,[2,*] and Simon Edvardson[4,5]

Progressive childhood encephalopathy is an etiologically heterogeneous condition characterized by progressive central nervous system dysfunction in association with a broad range of morbidity and mortality. The causes of encephalopathy can be either non-genetic or genetic. Identifying the genetic causes and dissecting the underlying mechanisms are critical to understanding brain development and improving treatments. Here, we report that variants in *TRAPPC12* result in progressive childhood encephalopathy. Three individuals from two unrelated families have either a homozygous deleterious variant (c.145delG [p.Glu49Argfs*14]) or compound-heterozygous variants (c.360dupC [p.Glu121Argfs*7] and c.1880C>T [p. Ala627Val]). The clinical phenotypes of the three individuals are strikingly similar: severe disability, microcephaly, hearing loss, spasticity, and characteristic brain imaging findings. Fibroblasts derived from all three individuals showed a fragmented Golgi that could be rescued by expression of wild-type TRAPPC12. Protein transport from the endoplasmic reticulum to and through the Golgi was delayed. TRAPPC12 is a member of the TRAPP protein complex, which functions in membrane trafficking. Variants in several other genes encoding members of the TRAPP complex have been associated with overlapping clinical presentations, indicating shared and distinct functions for each complex member. Detailed understanding of the TRAPPopathies will illuminate the role of membrane protein transport in human disease.

The combination of developmental regression, acquired microcephaly, and seizure disorder is consistent with the diagnosis of progressive childhood encephalopathy, which occurs at an overall cumulative incidence of 0.60 per 1,000 live births.[1] At the time of initial presentation, it is often impossible to determine whether encephalopathy is progressive, particularly in infants. Childhood encephalopathy can be caused by insults (hypoxia, hemorrhage, or toxins) or mutations in multiple genes associated with biochemical disorders and genetic syndromes. Both recessive and de novo dominant mechanisms have been described. In the absence of clear hypoxic or ischemic injury, history, clinical examination, and initial clinical testing often do not point to a specific diagnosis. Determining a diagnosis provides more precise prognostic information, prompts evaluations for associated complications, and increasingly guides specific treatment, particularly for biochemical disorders. For infants with encephalopathy, this information can be essential for medical decision making.

Genetic testing holds the promise of quickly identifying a specific cause for individuals with non-specific clinical presentations such as encephalopathy, but first, the genetic causes of these conditions must be identified and the associated clinical presentations must be described. The identification of encephalopathy-associated genes, via homozygosity mapping and candidate-gene sequencing, was progressing at a slow pace from 2000 to 2010. This has greatly accelerated in recent years thanks to the introduction of whole-exome sequencing (WES). As a result, remarkable advances are being made in the genetics of these early-onset neurodegenerative disorders.[2–7] A major challenge in WES analysis is identifying disease-associated variants among polymorphisms. Consanguinity, practiced by about 20% of the human population, including 31% of Israeli Arabs and 40% of Palestinian Arabs,[8,9] can facilitate the identification of candidate disease-related genes because of the presence of homozygous rare deleterious variants in affected individuals. Identifying compound-heterozygous variants in affected individuals from additional non-consanguineous families of different ethnicities further strengthens the evidence associating a gene with a specific disorder.

Here, we report variants in *TRAPPC12* (MIM: 614139) as a cause of progressive childhood encephalopathy on the basis of human genetic data from three affected individuals in two families (one consanguineous and one non-consanguineous). We further provide functional data showing changes in Golgi morphology, membrane-trafficking dysfunction, and mitotic delay in their fibroblasts.

Independently in Israel and the United States, we identified three affected individuals in two families with similar clinical features, including progressive encephalopathy, pons hypoplasia, agenesis of the corpus callosum, and brain atrophy (Table 1).

Procedures in this study were performed in accordance with the ethical standards of all institutions involved, and informed consent was obtained from all families.

[1]Department of Biology, Concordia University, Montreal, QC H4B 1R6, Canada; [2]Department of Pediatrics, University of Washington, Seattle, WA 98195, USA; [3]Department of Pathology, Center for Precision Diagnostics, University of Washington, Seattle, WA 98195, USA; [4]Monique and Jacques Roboh Department of Genetic Research, Hadassah-Hebrew University Medical Center, Jerusalem 91120, Israel; [5]Pediatric Neurology Unit, Hadassah-Hebrew University Medical Center, Jerusalem 91120, Israel; [6]Department of Anatomy and Cell Biology, McGill University, Montreal, QC H3A 0C7, Canada
*Correspondence: michael.sacher@concordia.ca (M.S.), ddoher@uw.edu (D.D.)
http://dx.doi.org/10.1016/j.ajhg.2017.07.006.

Table 1. Clinical Features of Individuals with *TRAPPC12*-Related Encephalopathy and Brain Atrophy

Features	1:II-8	2:II-1	2:II-4
Sex	male	female	female
Age	21 months	died at 4 years, 9 months	4 years, 8 months
Consanguinity	yes	no	no
Siblings	0	1 affected, 2 unaffected	1 affected, 2 unaffected
Screening for otoacoustic emissions (hearing loss)	failed	failed (40–60 dB)	failed (40–50 dB)
Presenting symptom (age)	seizures (5 months)	jittery (birth)	agenesis of the corpus callosum (prenatal)
Truncal hypotonia	yes	yes	yes
Appendicular spasticity	yes	yes	yes
Dystonia and/or myoclonus	yes	yes	yes
Eyes and/or vision	optic atrophy	mild optic nerve pallor and cortical visual impairment	enlarged cup/disk ratio, cortical visual impairment
Microcephaly	acquired	congenital	congenital
West syndrome	yes	no	no
Epilepsy	yes	yes	no
Global developmental delay	severe	severe	severe
Regression	yes	yes	yes
Neurogenic bladder	no	yes	no
Scoliosis	yes	yes	yes
Dysphagia and/or reflux	yes	yes (G-tube dependent)	yes (G-tube dependent)
Other	none	neonatal hypertension requiring amlodipine treatment, vocal cord paralysis	polyhydramnios, hip subluxation

In family 1, the 21-month-old affected boy (1:II-8) is the only living child of consanguineous Palestinian parents (Figure 1A). Five previous pregnancies ended in spontaneous abortions, a sixth pregnancy was terminated as a result of multiple anomalies, and a further child was born at 24 weeks of gestation and died soon after birth. Pregnancy and delivery of 1:II-8 were normal, as was the perinatal course, except that the individual failed neonatal hearing screening by otoacoustic emissions. Initial concerns regarding his development were raised at the age of 5 months, when the parents noted brief flexion seizures. Concomitantly, he stopped smiling, and visual tracking ceased. On examination at 6 months of age, truncal hypotonia, appendicular spasticity, microcephaly (40.2 cm, <-3 SD), and lack of response to social overtures were noted. On physical examination, no syndromic stigmata or other abnormalities were present. Initial electroencephalography (EEG) showed hypsarrhythmia (Figure S1) compatible with a diagnosis of West syndrome. His subsequent course was notable for a lack of psychomotor development, persistent epilepsy, and arrested head growth. Brain MRI was performed at 8 months of age and revealed pons hypoplasia, partial agenesis of the corpus callosum, and diffuse brain atrophy, as well as a relatively spared cerebellum (Figures 2A and 2E and Table 2). Extensive metabolic workup was negative; however, cerebrospinal fluid lactate was moderately elevated (3.2 mM, $N < 2.1$).

In family 2, the 32-year-old mother of 2:II-4 arrived at our prenatal diagnostic clinic after a maternal serum screen revealed a 1/55 risk of trisomy 18 and an outside ultrasound at an estimated 20 weeks of gestation revealed absent cavum septi pellucidi. Follow-up ultrasound and fetal MRI revealed agenesis of the corpus callosum but no other abnormal imaging findings. The family history was significant for a sister (2:II-1) with profound developmental disability, mixed hearing loss, seizures, and microcephaly (head circumference at -4 SD). The parents are nonconsanguineous (Figure 1B) and of mixed European and Native American background. Individual 2:II-4 was born by uncomplicated vaginal delivery at 36 weeks of gestation, and her newborn course was unremarkable except for minor feeding difficulties and the identification of pons hypoplasia and agenesis of the corpus callosum on brain MRI (Figure 2). She failed her newborn hearing screen and has documented bilateral 40–50 dB mixed hearing loss. Over time, 2:II-4 developed features similar to those of her sister (2:II-1), including spastic quadriplegia, myoclonic jerks, and severe disability. During infancy,

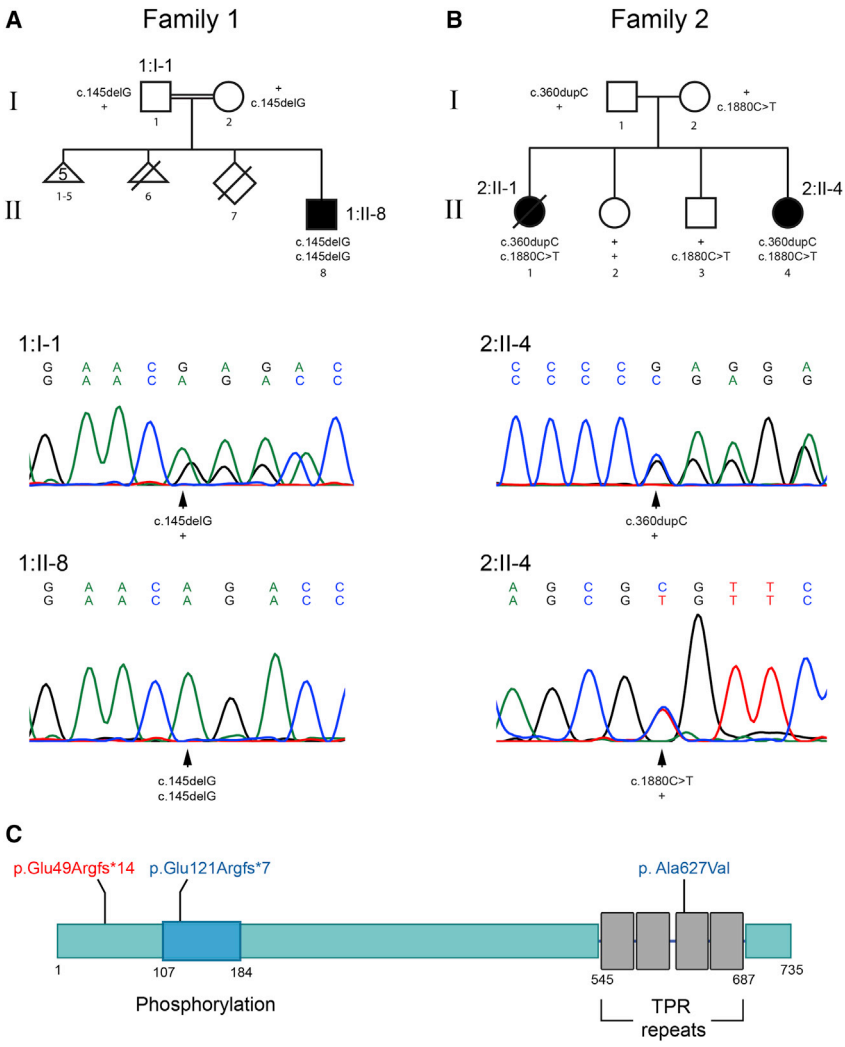

Figure 1. Pedigrees and Characterization of *TRAPPC12* Variants

(A and B) Pedigree structure for family 1 (A) and family 2 (B). Electropherograms are shown for affected regions in 1:I-1 (carrier father), 1:II-8 (affected), and 2:II-4 (affected). Note that the heterozygous variant c.145delG in the proband's father (1:I-1) results in a mixture of bases from that region onward but not in 1:II-8. Similarly, 2:II-1 and 2:II-4 have the frameshift variant c.360dupC, resulting in a mixture of nucleotides from the point of insertion, as well as the missense c.1880C>T.

(C) A cartoon of the structure of TRAPPC12 with known domains and the locations of the variants in 1:II-8 (red) and 2:II-1 and 2:II-4 (blue). Note that phosphorylation indicates a region of phosphorylation known to affect mitosis.[10]

both girls made small developmental gains such as tracking and smiling but then plateaued. Before her demise from presumed respiratory insufficiency at 4 years 9 months, 2:II-1 developed seizures, increasing spasticity, and a neurogenic bladder. Review of brain imaging for all three affected individuals revealed remarkably similar findings, including pons hypoplasia, agenesis of the corpus callosum, and marked brain atrophy documented by scans from 3 days to 11 months of age (Figure 2 and Table 2).

We performed exome sequencing of the affected individual in family 1 (1:II-8) and the two affected individuals in family 2 (2:II-1 and 2:II-4) and analyzed the data under a recessive model. Exome analysis of 1:II-8 yielded 75.5 million mapped reads with a mean coverage of 129×. After alignment to the reference genome (UCSC Genome Browser hg19) and variant calling, we performed a series of filtering steps. These included removing variants that were called fewer than eight times, were heterozygous, were synonymous, and had a minor allele frequency (MAF) > 1% in the ExAC (Exome Aggregation Consortium) Browser or MAF > 1% in the Hadassah in-house database. A total of 15 variants remained (Table S1), but using evolutionary conservation, the presence of homozygotes in the ExAC Browser, and pathogenicity-prediction software, we focused on chr2: g.3391539delG (c.145delG; p.Glu49Argfs*14) (GenBank: NM_016030.5) in *TRAPPC12*. We confirmed homozygosity in the individual and heterozygosity in the parents by Sanger sequencing. The variant was not carried by any of the 49,094 individuals whose exome analyses were deposited in the ExAC Browser (accessed September 2016) and covered the gene, and it was not present in our in-house database (of ~850 Muslim-Arab exome analyses).

In parallel, individuals 2:II-1 and 2:II-4 were sequenced with a mean coverage of 188× and 211×, respectively. We filtered out variants with an MAF > 1% in the ExAC Browser and prioritized genes with two stop-gain, frameshift, canonical splice-site, or predicted-deleterious missense variants in both siblings. The variants in *TRAPPC12* and *DOPEY2* (MIM: 604803) met these criteria (Table S1). *TRAPPC12* was our top candidate because it contained frameshift variant chr2: g.3391754_3391755insC (c.360dupC; p.Glu121Argfs*7) (GenBank: NM_016030.5) and predicted-deleterious missense variant chr2: g.3482619C>T (c.1880C>T; p. Ala627Val) (GenBank: NM_016030.5), whereas *DOPEY2* contained two missense variants, and because the phenotype was nearly identical to that of individual 1:II-8, who carries the homozygous frameshift variant. Sanger sequencing confirmed the *TRAPPC12* variants in both affected siblings, whereas the father carries the frameshift variant and the mother carries the missense variant. Neither of the unaffected siblings carries both variants. It is noteworthy that gnomAD lists two instances of p.Ala627Val and eight instances of p.Ala627Thr among 246,176 alleles,

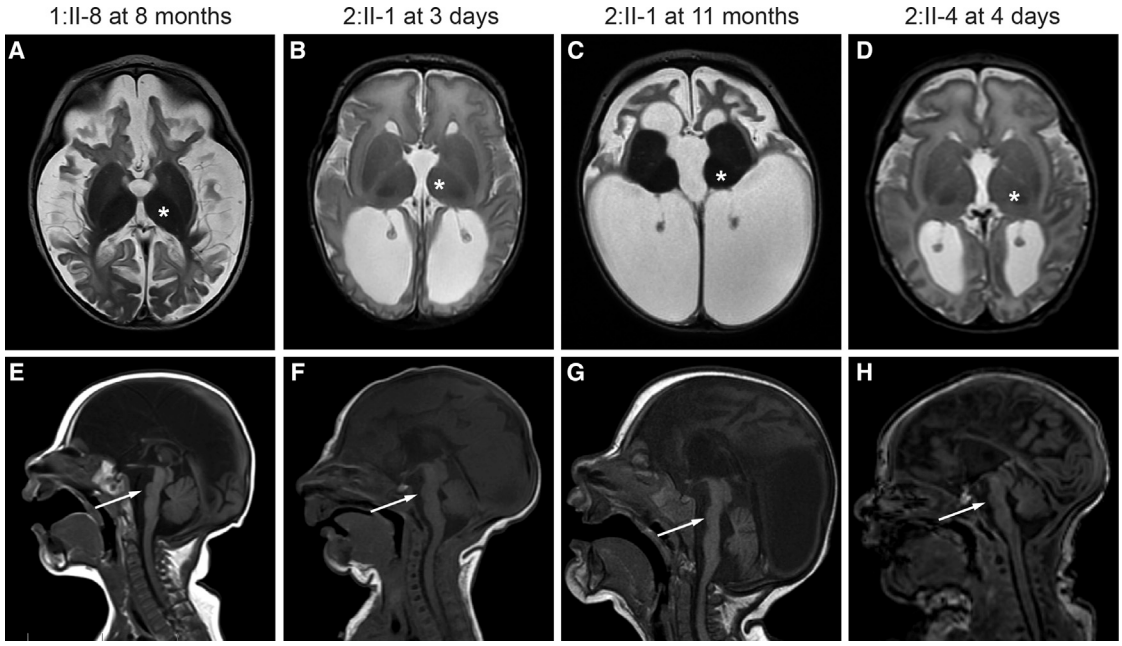

Figure 2. Brain Imaging Features of Individuals with *TRAPPC12*-Related Encephalopathy and Brain Atrophy
(A–D) T2-weighted axial images show that all three affected individuals have severely atrophic-appearing cortex (white and gray matter). Documented volume loss was noted between 3 days (B) and 11 months (C) of age in 2:II-1. T2 signal is increased in the white matter, consistent with decreased myelination. Basal ganglia volume is relatively spared (asterisks). 2:II-4 also has progressive ventriculomegaly beyond what would be expected for cortical volume loss but did not have overt symptoms of increased intracranial pressure.
(E–H) T1-weighted sagittal images show severe pons hypoplasia (arrows) and agenesis of the corpus callosum, as well as relative sparing of the cerebellum.

well within the range of carrier frequencies expected for a very rare disorder.

TRAPPC12 was identified as a component of a large complex called TRAPP, which functions in membrane trafficking between the endoplasmic reticulum (ER) and the Golgi.[11] As expected for the homozygous truncating variant in 1:II-8, western blot analysis failed to detect any full-length TRAPPC12 (Figure 3A). Unexpectedly, the full-length protein was also absent in 2:II-1 and 2:II-4, in whom one allele is predicted to result in the missense change p.Ala627Val. In all three affected individuals, an increase in the proportion of cells with a fragmented Golgi was noted (Figure 3B and quantified in Figure 3D), consistent with the fragmentation reported in HeLa cells when TRAPPC12 was depleted by RNA interference.[10,11] In order to confirm that the Golgi phenotype was indeed due to the loss of TRAPPC12, we transfected fibroblasts with a V5-tagged wild-type TRAPPC12 and visualized the Golgi in the transfected and non-transfected cells. As seen in Figure 3C and quantified in Figure 3D, transfected cells from affected individuals displayed a more ribbon-like, compact pattern for the Golgi than did non-transfected cells, suggesting that the fragmented Golgi phenotype is due to the absence of TRAPPC12. Recently, TRAPPC12 was reported to play a role in mitosis, and depletion of the protein in HeLa cells resulted in a chromosome congression failure.[10] Therefore, we assessed the timing of mitosis between fibroblasts derived from all three affected individuals and those from control samples. Indeed, 1:II-8, 2:II-1, and 2:II-4 showed a significant lengthening of the time from prophase until the onset of anaphase (Figure 3E).

We then used live-cell imaging to track the movement of a marker protein (VSVG-GFP-ts045) from the ER through the Golgi and on to the plasma membrane.[13] This protein remains trapped in the ER at elevated temperature (40°C) and can be released in a single wave of export when the culture temperature is lowered (32°C). The marker protein's entrance into and exit from the Golgi can be monitored by quantification of the fluorescent signal in the Golgi over time. As shown in Figure 4A, VSVG-GFP-ts045 was transported from the ER to the fragmented Golgi in all three affected individuals. Quantification of the fluorescence signal (Figure 4B) suggested that the protein arrived in the Golgi slightly later in 1:II-8, 2:II-1, and 2:II-4 cells than in wild-type fibroblasts. The protein then remained in the Golgi of 1:II-8, 2:II-1, and 2:II-4 cells longer than in control cells. These results are consistent with those reported for variants in another TRAPP subunit, TRAPPC11.[14,15] To confirm and better assess the ER-to-Golgi delay, we employed the RUSH (retention using selective hooks) assay, in which the Golgi marker protein is retained in the ER via an interaction that can be reversed upon the addition of biotin.[16] As shown in Figure 4C and quantified in Figure 4D, fibroblasts from all three affected individuals showed later arrival of the marker protein in the Golgi than did control cells.

Table 2. Brain Imaging Features of Individuals with *TRAPPC12*-Related Encephalopathy and Brain Atrophy

MRI Feature	1:II-8	2:II-1	2:II-4
Age at MRI	8 months	3 days, 11 months	4 days
Severe cortical atrophy	yes	yes	yes
Ventriculomegaly	yes	yes	yes
Prominent extra-axial spaces	yes	yes	yes
Simplified frontal gyri	yes	yes	yes
Increased T2 signal in cortical white matter	yes	yes	yes
Agenesis of the corpus callosum	severe thinning with absent posterior body, isthmus, and splenium	complete absence	severe thinning with absent posterior body, isthmus, and splenium
Relatively spared basal ganglia	yes	yes	yes
Small optic chiasm	yes	yes	no
Severe pons hypoplasia	yes	yes	yes
Cerebellar hypoplasia	no	mild	mild
Other	none	high T2 signal in optic chiasm, bilateral cerebellar hemorrhage, effacement of the posterior extra-axial spaces	unilateral cerebellar hemorrhage

Herein, we have identified three individuals in two families with bi-allelic, rare predicted-deleterious variants in *TRAPPC12*, a gene that encodes a subunit of the TRAPP complex. All three individuals have severe neurodevelopmental disability, hearing loss, microcephaly, and a recognizable constellation of brain imaging findings, including pons hypoplasia, agenesis of the corpus callosum, and supratentorial atrophy. Although it is not possible to generalize the phenotypic presentation on the basis of three individuals, the constellation of congenital encephalopathy, hearing loss, pons hypoplasia, and prominent supratentorial atrophy is unusual and should prompt evaluation of deleterious *TRAPPC12* variants in single-gene, panel, or exome-sequencing data. *TRAPPC12* could be included in sequencing panels for neonatal encephalopathies, hearing loss, pontocerebellar hypoplasia, and brain atrophy disorders.

The symptoms described above for all three individuals are most likely a result of the lack of TRAPPC12. The complete absence of full-length TRAPPC12 from 2:II-1 and 2:II-4 (Figure 3A) can have several explanations. Although the c.360dupC allele would be predicted to result in a prematurely truncated protein, the c.1880 C>T allele is predicted to result in only a conservative p.Ala627Val missense variant. This alanine residue is at position 8 of the third tetratricopeptide repeat (TPR) domain (Figure 1C). TPR domains are composed of a degenerate 34 amino acid primary structure in which several residues are key, including position 8, which is nearly invariably alanine, glycine, or serine.[17,18] Changing this residue to a bulky valine would be predicted to have deleterious effects on the function and/or structure of this domain. The absence of the protein could be due to its instability with valine at position 627 and degradation via the proteasome. Interestingly, treatment of fibroblasts from 2:II-1 and 2:II-4 with the proteasome inhibitor MG-132 did not result in the appearance of the full-length protein (data not shown). Furthermore, decreased gene expression does not explain the absence of TRAPPC12, given that the mRNA for 2:II-1 and 2:II-4 was present at 68.3% (±3.3) and 72.0% (±3.4), respectively, of control levels according to qPCR. Understanding the reason for the lack of protein in these individuals will be the subject of further investigation.

One of the two mothers (1:I-2) had recurrent spontaneous abortions and premature labor. In addition to playing a role in ER-Golgi transport, TRAPPC12 has been recently reported to also function in mitosis.[10] Its depletion caused activation of the spindle assembly checkpoint and affected the structure of the kinetochore and the recruitment of CENP-E. It is tempting to speculate that this role of TRAPPC12 was affected at an early stage of the pregnancy. Alternatively, *TRAPPC12* haploinsufficiency might have a detrimental effect on the ability of the mother to carry an embryo to full term. In this regard, it is noteworthy that the levels of the TRAPP subunit TRAPPC2 have been implicated in miscarriage.[19]

The TRAPP complex was discovered first in yeast as a multi-subunit vesicle-tethering complex. Yeast have three TRAPP complexes: TRAPP I, implicated in ER-to-Golgi transport;[20] TRAPP II, implicated in late Golgi trafficking;[21] and TRAPP III, implicated in autophagy.[22,23] All three complexes share a common core of subunits and additional TRAPP II- and TRAPP III-specific subunits.[24] In mammals, two TRAPP complexes have been described, and they are equivalent to the yeast TRAPP II and TRAPP III complexes,[25] which function at ER exit sites

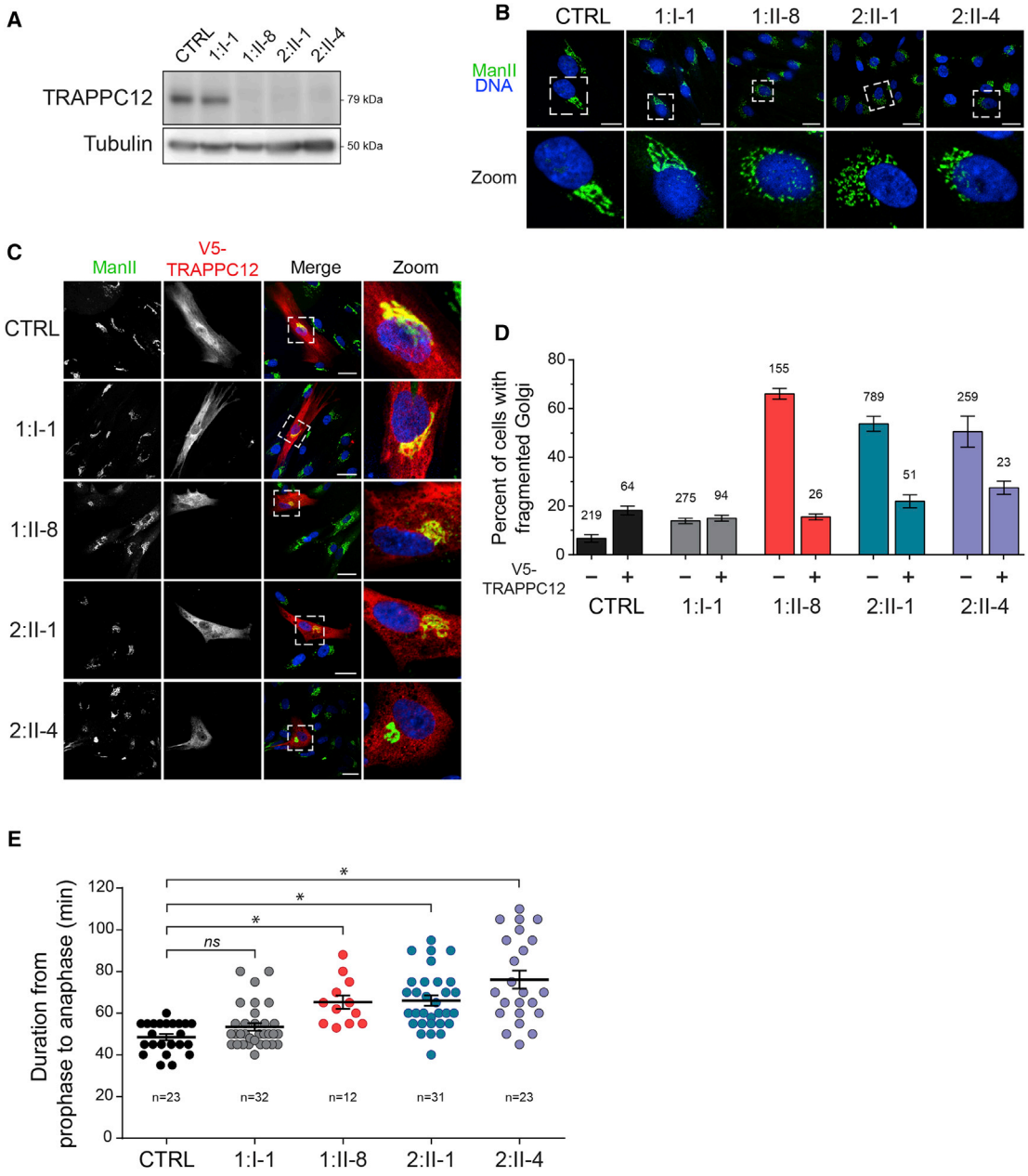

Figure 3. The Absence of *TRAPPC12* from Fibroblasts Results in Changes to Golgi Morphology and Delays in Mitosis

(A) Lysates from fibroblasts derived from a control sample (CTRL), the heterozygous father (1:I-1), 1:II-8, and the compound-heterozygous individuals 2:II-1 and 2:II-4 were probed for TRAPPC12 by western analysis. A tubulin loading control is also shown.

(B) Control, 1:I-1, 1:II-8, 2:II-1, and 2:II-4 fibroblasts were processed for immunofluorescence microscopy and stained for the Golgi marker mannosidase II (Man II) and Hoechst (Invitrogen) to reveal the nucleus. Note the more fragmented Golgi in fibroblasts from affected individuals. Fragmentation is quantified in (D). Scale bars, 25 μm.

(C) Control, 1:I-1, 1:II-8, 2:II-1, and 2:II-4 fibroblasts were transfected by electroporation with a V5-tagged wild-type TRAPPC12 construct. Cells were then processed for immunofluorescence microscopy and stained as in (B), except that anti-V5 antibody was also used to reveal the TRAPPC12-transfected cells. Note the more compact Golgi in the transfected cells than in the neighboring non-transfected cell. Scale bars, 25 μm.

(D) Golgi fragmentation in non-transfected cells from (B) and (C) and V5-TRAPPC12-transfected cells from (C) were quantified (±SEM). Golgi fragmentation was based upon the criteria stated previously.[12] The numbers above each bar represent N values.

(E) Fibroblasts were grown in the presence of 75 nM SiR-tubulin (Cytoskeleton, Inc.) for 3 hr and 50 ng/mL Hoechst (to label DNA) for the final 15 min before visualization by real-time microscopy overnight. Cells that underwent mitosis during imaging were quantified (±SEM) by assessment of the time between prophase and anaphase. Prophase was defined by the appearance of condensed DNA with two centrioles at opposite poles, and anaphase was defined as the initial separation of the aligned metaphase DNA. Significance was assessed between wild-type and each subject by a one way ANOVA. Post hoc differences were made with Fisher's probability of least squared differences. p values ≤ 0.01 are indicated by an asterisk.

The antibodies used in this figure were (A) anti-TRAPPC12 (generated in house to full-length recombinant protein) and anti-tubulin (Sigma, DM1A), (B and C) anti-mannosidase II (kind gift from Dr. Kelly Moremen, University of Georgia), and (C) anti-V5 (Abcam, ab27671).

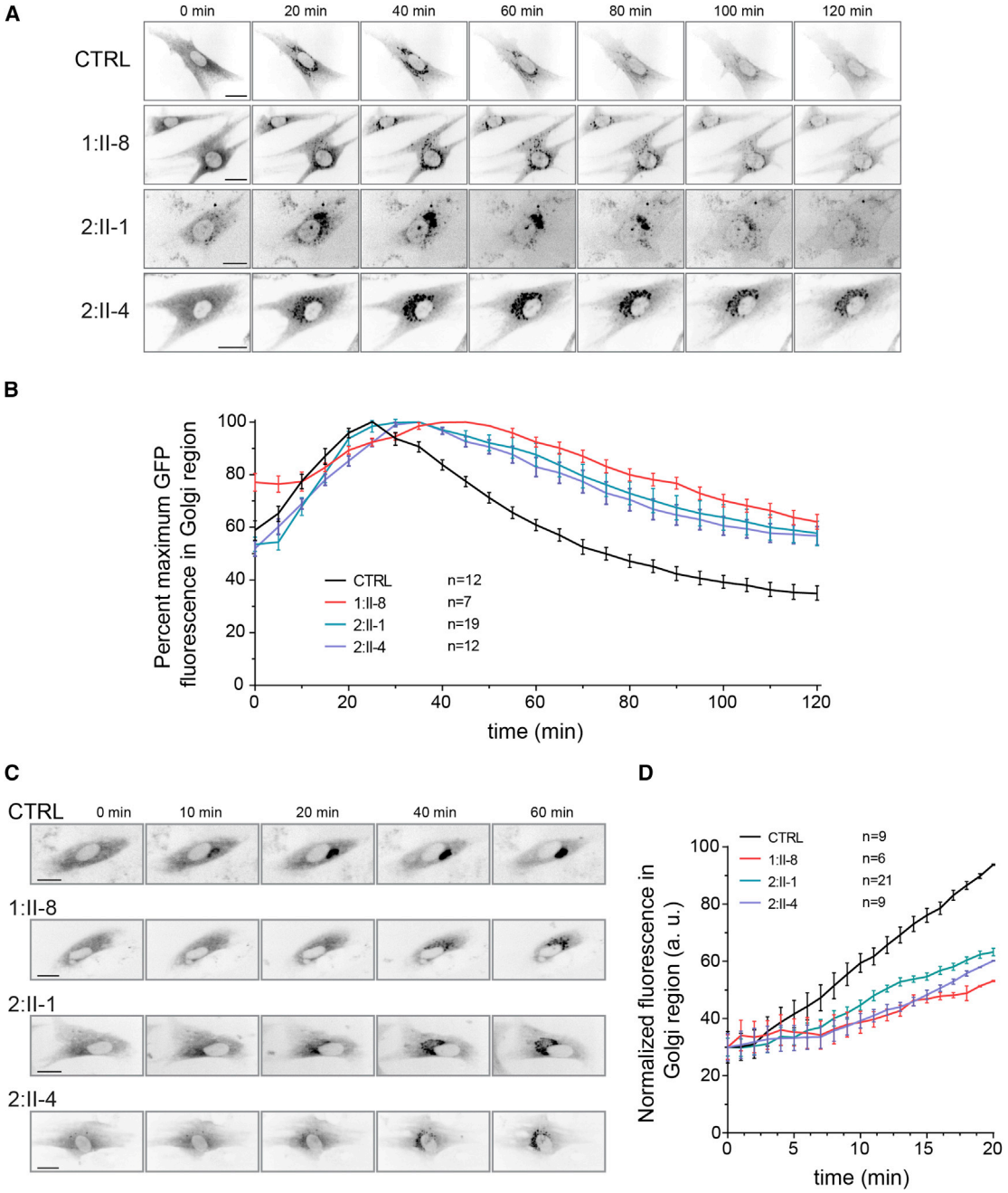

Figure 4. Trafficking into and out of the Golgi Is Delayed in Subjects with TRAPPC12 Variants
(A) Control, 1:II-8, 2:II-1, and 2:II-4 fibroblasts were infected with an adenovirus that expresses VSVG-GFP ts045 marker protein (kind gift from Dr. Martin Lowe, University of Manchester) and maintained overnight at 40°C for trapping the marker protein in the ER. The culture was then shifted to 32°C to release the marker protein from the ER. Cells were imaged over a 2 hr period. Still images from the live-cell imaging at the times indicated are presented. Scale bars, 25 μm.
(B) The fluorescence intensity in the Golgi region from individual cells in (A) was measured every 5 min and plotted (±SEM) as the mean percentage of maximal intensity.
(C) Fibroblasts from a control sample, 1:II-8, 2:II-1, and 2:II-4 were transfected with a plasmid that expresses both sialyl transferase (ST)-GFP fused to a streptavidin binding protein and an ER-resident protein fused to streptavidin. The addition of 50 μM biotin resulted in the release of ST-GFP from the ER, and its appearance in the Golgi was followed in real time over a 1 hr period. Scale bars, 25 μm.
(D) The fluorescence intensity in the Golgi region from individual cells in (C) was calculated every 60 s and plotted (±SEM) as the mean percentage of maximal intensity.

and in autophagy.[11,26] The mammalian complexes (reviewed in Kim et al.[27]) are composed of at least 13 distinct polypeptides (C1–C6a, C6b, and C8–C13), and disease-causing variants were recently described in three of them. Bi-allelic variants in *TRAPPC11* (MIM: 614138) have been reported in individuals with intellectual

disability, movement disorder, premature cataracts, steatosis, achalasia, alacrima, scoliosis, and muscular dystrophy;[14,15,28] variants in *TRAPPC2* (MIM: 300202) have been described in individuals with an X-linked skeletal disorder;[29] and variants in *TRAPPC9* (MIM: 611966) have been reported in individuals with autosomal-recessive intellectual disability.[30]

The present study now adds a fourth TRAPP subunit gene, *TRAPPC12*, to the growing list of genes involved in TRAPP-opathies. The variants (homozygous and compound heterozygous) result in complete loss of full-length TRAPPC12 and are associated with fragmentation of the Golgi, similar to what was observed in HeLa cells upon knockdown of the protein.[10,11] Alterations of the Golgi apparatus are accompanied by loss or gain of function in protein sorting, processing and transport, and activation of apoptotic pathways.[31] It is noteworthy that Golgi fragmentation is commonly observed in several neurodegenerative disorders, although a cause-and-effect relationship is still unknown.[32] Defects in subunits of the conserved oligomeric Golgi complex (required for intra-Golgi trafficking) and clathrin (a component of the clathrin coat involved in endocytosis), as well as proteins important in the docking and fusion of endosomal vesicles, were previously associated with progressive childhood encephalopathy (reviewed in Edvardson et al.[33] and Reynders et al.[34]).

Delineating the genetic causes of childhood encephalopathies has important implications for prognostic and recurrence risk counseling, diagnostic and carrier testing, medical monitoring for complications, and treatment. In addition, these human disorders are helping to dissect the function of fundamental cellular processes, such as protein trafficking, and will have wide-reaching implications for developing future treatments that target these processes.

Accession Numbers

The accession numbers for the *TRAPPC12* variants reported in this paper are ClinVar: SCV000583603 and SCV000583604.

Supplemental Data

Supplemental Data include one figure and one table and can be found with this article online at http://dx.doi.org/10.1016/j.ajhg.2017.07.006.

Acknowledgments

We thank the families for participating in this study. This work was supported by funding from the Canadian Institutes of Health Research (M.S.), the Natural Sciences and Engineering Research Council of Canada (M.S.), the Trudy Mandel Louis Charitable Trust (O.E.), the University of Washington Pediatrics Department (D.D.), and the NIH Eunice Kennedy Shriver National Institute of Child Health and Human Development U54HD083091 Genetics Core (D.D.). The M.S. laboratory is a member of the Groupe de Recherche Axé sur la Structure des Protéines. S.E. completed this work while on sabbatical.

Dedication: this paper is dedicated to the memory of Jessica Yudcovitch, a young woman who was full of life, kindness, generosity, and love and who accomplished so much in her brief lifetime. May the memory of her laughter and smile be a comfort for her family and friends.

Received: May 1, 2017
Accepted: July 6, 2017
Published: August 3, 2017

Web Resources

ExAC Browser, http://exac.broadinstitute.org
GenBank, https://www.ncbi.nlm.nih.gov/genbank/
gnomAD browser, http://gnomad.broadinstitute.org/
OMIM, http://www.omim.org
UCSC Genome Browser, https://genome.ucsc.edu/

References

1. Stromme, P., Kanavin, O.J., Abdelnoor, M., Woldseth, B., Rootwelt, T., Diderichsen, J., Bjurulf, B., Sommer, F., and Magnus, P. (2007). Incidence rates of progressive childhood encephalopathy in Oslo, Norway: a population based study. BMC Pediatr. *7*, 25–32.
2. Armstrong, L., Biancheri, R., Shyr, C., Rossi, A., Sinclair, G., Ross, C.J., Tarailo-Graovac, M., Wasserman, W.W., and van Karnebeek, C.D. (2014). AIMP1 deficiency presents as a cortical neurodegenerative disease with infantile onset. Neurogenetics *15*, 157–159.
3. Chong, J.X., Caputo, V., Phelps, I.G., Stella, L., Worgan, L., Dempsey, J.C., Nguyen, A., Leuzzi, V., Webster, R., Pizzuti, A., et al.; University of Washington Center for Mendelian Genomics (2016). Recessive Inactivating Mutations in TBCK, Encoding a Rab GTPase-Activating Protein, Cause Severe Infantile Syndromic Encephalopathy. Am. J. Hum. Genet. *98*, 772–781.
4. Dimassi, S., Labalme, A., Ville, D., Calender, A., Mignot, C., Boutry-Kryza, N., de Bellescize, J., Rivier-Ringenbach, C., Bourel-Ponchel, E., Cheillan, D., et al. (2016). Whole-exome sequencing improves the diagnosis yield in sporadic infantile spasm syndrome. Clin. Genet. *89*, 198–204.
5. Kurata, H., Terashima, H., Nakashima, M., Okazaki, T., Matsumura, W., Ohno, K., Saito, Y., Maegaki, Y., Kubota, M., Nanba, E., et al. (2016). Characterization of SPATA5-related encephalopathy in early childhood. Clin. Genet. *90*, 437–444.
6. Mandel, H., Khayat, M., Chervinsky, E., Elpeleg, O., and Shalev, S. (2017). TBCK-related intellectual disability syndrome: Case study of two patients. Am. J. Med. Genet. A. *173*, 491–494.
7. Nakashima, M., Takano, K., Tsuyusaki, Y., Yoshitomi, S., Shimono, M., Aoki, Y., Kato, M., Aida, N., Mizuguchi, T., Miyatake, S., et al. (2016). WDR45 mutations in three male patients with West syndrome. J. Hum. Genet. *61*, 653–661.
8. Sharkia, R., Mahajnah, M., Athamny, E., Khatib, M., Sheikh-Muhammad, A., and Zalan, A. (2016). Changes in marriage patterns among the Arab community in Israel over a 60-year period. J. Biosoc. Sci. *48*, 283–287.

9. Sirdah, M.M. (2014). Consanguinity profile in the Gaza Strip of Palestine: large-scale community-based study. Eur. J. Med. Genet. *57*, 90–94.
10. Milev, M.P., Hasaj, B., Saint-Dic, D., Snounou, S., Zhao, Q., and Sacher, M. (2015). TRAMM/TrappC12 plays a role in chromosome congression, kinetochore stability, and CENP-E recruitment. J. Cell Biol. *209*, 221–234.
11. Scrivens, P.J., Noueihed, B., Shahrzad, N., Hul, S., Brunet, S., and Sacher, M. (2011). C4orf41 and TTC-15 are mammalian TRAPP components with a role at an early stage in ER-to-Golgi trafficking. Mol. Biol. Cell *22*, 2083–2093.
12. Scrivens, P.J., Shahrzad, N., Moores, A., Morin, A., Brunet, S., and Sacher, M. (2009). TRAPPC2L is a novel, highly conserved TRAPP-interacting protein. Traffic *10*, 724–736.
13. Scales, S.J., Pepperkok, R., and Kreis, T.E. (1997). Visualization of ER-to-Golgi transport in living cells reveals a sequential mode of action for COPII and COPI. Cell *90*, 1137–1148.
14. Bögershausen, N., Shahrzad, N., Chong, J.X., von Kleist-Retzow, J.C., Stanga, D., Li, Y., Bernier, F.P., Loucks, C.M., Wirth, R., Puffenberger, E.G., et al. (2013). Recessive TRAPPC11 mutations cause a disease spectrum of limb girdle muscular dystrophy and myopathy with movement disorder and intellectual disability. Am. J. Hum. Genet. *93*, 181–190.
15. Koehler, K., Milev, M.P., Prematilake, K., Reschke, F., Kutzner, S., Jühlen, R., Landgraf, D., Utine, E., Hazan, F., Diniz, G., et al. (2017). A novel TRAPPC11 mutation in two Turkish families associated with cerebral atrophy, global retardation, scoliosis, achalasia and alacrima. J. Med. Genet. *54*, 176–185.
16. Boncompain, G., Divoux, S., Gareil, N., de Forges, H., Lescure, A., Latreche, L., Mercanti, V., Jollivet, F., Raposo, G., and Perez, F. (2012). Synchronization of secretory protein traffic in populations of cells. Nat. Methods *9*, 493–498.
17. D'Andrea, L.D., and Regan, L. (2003). TPR proteins: the versatile helix. Trends Biochem. Sci. *28*, 655–662.
18. Sikorski, R.S., Boguski, M.S., Goebl, M., and Hieter, P. (1990). A repeating amino acid motif in CDC23 defines a family of proteins and a new relationship among genes required for mitosis and RNA synthesis. Cell *60*, 307–317.
19. Wen, J., Hanna, C.W., Martell, S., Leung, P.C., Lewis, S.M., Robinson, W.P., Stephenson, M.D., and Rajcan-Separovic, E. (2015). Functional consequences of copy number variants in miscarriage. Mol. Cytogenet. *8*, 6–14.
20. Sacher, M., Barrowman, J., Wang, W., Horecka, J., Zhang, Y., Pypaert, M., and Ferro-Novick, S. (2001). TRAPP I implicated in the specificity of tethering in ER-to-Golgi transport. Mol. Cell *7*, 433–442.
21. Cai, H., Zhang, Y., Pypaert, M., Walker, L., and Ferro-Novick, S. (2005). Mutants in trs120 disrupt traffic from the early endosome to the late Golgi. J. Cell Biol. *171*, 823–833.
22. Lynch-Day, M.A., Bhandari, D., Menon, S., Huang, J., Cai, H., Bartholomew, C.R., Brumell, J.H., Ferro-Novick, S., and Klionsky, D.J. (2010). Trs85 directs a Ypt1 GEF, TRAPPIII, to the phagophore to promote autophagy. Proc. Natl. Acad. Sci. USA *107*, 7811–7816.
23. Meiling-Wesse, K., Epple, U.D., Krick, R., Barth, H., Appelles, A., Voss, C., Eskelinen, E.L., and Thumm, M. (2005). Trs85 (Gsg1), a component of the TRAPP complexes, is required for the organization of the preautophagosomal structure during selective autophagy via the Cvt pathway. J. Biol. Chem. *280*, 33669–33678.
24. Brunet, S., and Sacher, M. (2014). In sickness and in health: the role of TRAPP and associated proteins in disease. Traffic *15*, 803–818.
25. Bassik, M.C., Kampmann, M., Lebbink, R.J., Wang, S., Hein, M.Y., Poser, I., Weibezahn, J., Horlbeck, M.A., Chen, S., Mann, M., et al. (2013). A systematic mammalian genetic interaction map reveals pathways underlying ricin susceptibility. Cell *152*, 909–922.
26. Lamb, C.A., Nühlen, S., Judith, D., Frith, D., Snijders, A.P., Behrends, C., and Tooze, S.A. (2016). TBC1D14 regulates autophagy via the TRAPP complex and ATG9 traffic. EMBO J. *35*, 281–301.
27. Kim, J.J., Lipatova, Z., and Segev, N. (2016). TRAPP Complexes in Secretion and Autophagy. Front. Cell Dev. Biol. *4*, 20–30.
28. Liang, W.C., Zhu, W., Mitsuhashi, S., Noguchi, S., Sacher, M., Ogawa, M., Shih, H.H., Jong, Y.J., and Nishino, I. (2015). Congenital muscular dystrophy with fatty liver and infantile-onset cataract caused by TRAPPC11 mutations: broadening of the phenotype. Skelet. Muscle *5*, 29–34.
29. Gedeon, A.K., Colley, A., Jamieson, R., Thompson, E.M., Rogers, J., Sillence, D., Tiller, G.E., Mulley, J.C., and Gécz, J. (1999). Identification of the gene (SEDL) causing X-linked spondyloepiphyseal dysplasia tarda. Nat. Genet. *22*, 400–404.
30. Mir, A., Kaufman, L., Noor, A., Motazacker, M.M., Jamil, T., Azam, M., Kahrizi, K., Rafiq, M.A., Weksberg, R., Nasr, T., et al. (2009). Identification of mutations in TRAPPC9, which encodes the NIK- and IKK-beta-binding protein, in nonsyndromic autosomal-recessive mental retardation. Am. J. Hum. Genet. *85*, 909–915.
31. Machamer, C.E. (2015). The Golgi complex in stress and death. Front. Neurosci. *9*, 421–425.
32. Rabouille, C., and Haase, G. (2016). Editorial: Golgi Pathology in Neurodegenerative Diseases. Front. Neurosci. *9*, 489–491.
33. Edvardson, S., Cinnamon, Y., Ta-Shma, A., Shaag, A., Yim, Y.I., Zenvirt, S., Jalas, C., Lesage, S., Brice, A., Taraboulos, A., et al. (2012). A deleterious mutation in DNAJC6 encoding the neuronal-specific clathrin-uncoating co-chaperone auxilin, is associated with juvenile parkinsonism. PLoS ONE *7*, e36458.
34. Reynders, E., Foulquier, F., Annaert, W., and Matthijs, G. (2011). How Golgi glycosylation meets and needs trafficking: the case of the COG complex. Glycobiology *21*, 853–863.

The American Journal of Human Genetics, Volume *101*

Supplemental Data

Mutations in *TRAPPC12* Manifest in Progressive Childhood Encephalopathy and Golgi Dysfunction

Miroslav P. Milev, Megan E. Grout, Djenann Saint-Dic, Yong-Han Hank Cheng, Ian A. Glass, Christopher J. Hale, David S. Hanna, Michael O. Dorschner, Keshika Prematilake, Avraham Shaag, Orly Elpeleg, Michael Sacher, Dan Doherty, and Simon Edvardson

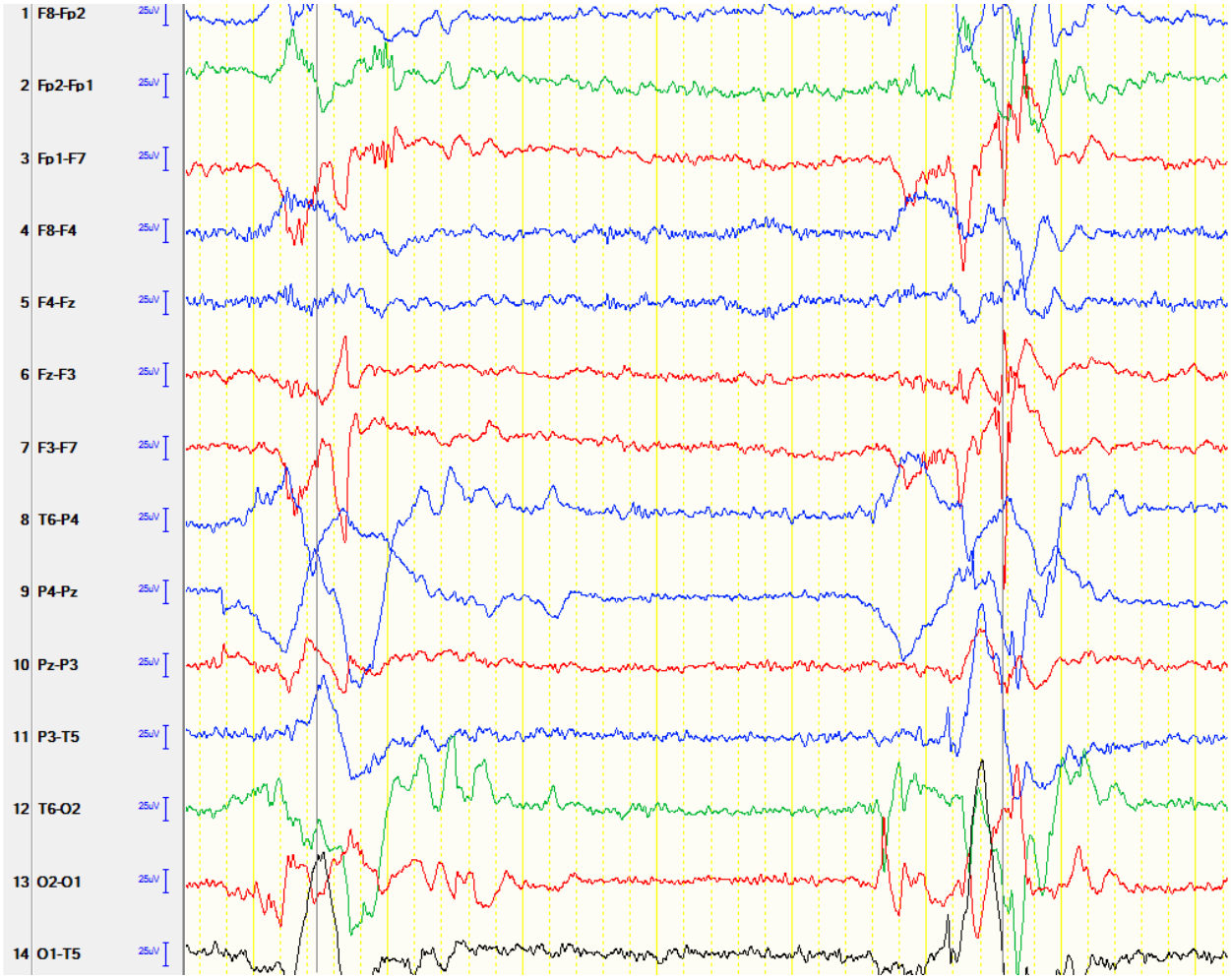

Figure S1. EEG at six months of age in 1:II-8 shows disorganized background activity with multifocal and generalized epileptiform activity consistent with hypsarrhythmia.

Table S1. Candidate recessive genetic causes based on exome sequencing in families F4331 and UW336

F4331 Family											
Chr	**bp (hg19)**	**ref**	**alt**	**gene**	**cDNA change**	**AA change**	**ExAC MAF**	**GERP**	**CADD**	**MT**	**rs**
2	3391538	CG	C	*TRAPPC12*	NM_016030.5:c.145del	p.Glu49Argfs*14	NR	5.00	16.18	D	NR
3	126070876	C	A	*KLF15*	NM_014079.3:c.890G>T	p.Gly297Val	NR	4.25	10.94	D	NR
3	126722227	G	A	*PLXNA1*	NM_032242.3:c.1432G>A	p.Val478Ile	0.0008	4.43	17.75	D	rs199693063
3	148601571	C	T	*CPA3*	NM_001870.2:c.950C>T	p.Thr317Ile	0.0018	4.77	20.2	D	rs142588358
5	56155651	G	A	*MAP3K1*	NM_005921.1:c.743G>A	p.Arg248Gln	0.0002	5.72	20.5	D	rs201579608
7	111926991	T	C	*ZNF277*	NM_021994.2:c.155T>C	p.Leu52Ser	0.000008	1.97	13.74	P	rs764056350
8	10467637	T	C	*RP1L1*	NM_178857.5:c.3971A>G	p.Glu1324Gly	NR	-1.85	6.54	P	rs4240659
12	49725054	T	C	*TROAP*	NM_005480.3:c.2156T>C	p.Leu719Ser	0.0001	4.73	17.59	P	rs545155075
13	52676340	T	C	*NEK5*	NM_199289.1:c.698A>G	p.His233Arg	0.004	-7.44	0.009	P	rs56369842
13	52710344	C	T	*NEK3*	NM_001146099.1:c.1031G>A	p.Arg344Gln	0.0016	0.85	8.65	P	rs74087069
X	48460322	G	A	*WDR13*	NM_017883.4:c.982G>A	p.Val328Ile	0.0005	3.65	0.18	P	rs150193416
X	63409994	G	A	*AMER1*	NM_152424.3:c.3173C>T	p.Pro1058Leu	0.00002	4.83	17.58	D	rs760083711
X	73641702	C	A	*SLC16A2*	NM_006517.4:c.230C>A	p.Pro77His	NR	2.24	12.49	P	NR
X	101139020	T	G	*ZMAT1*	NM_001011657.3:c.1379A>C	p.Gln460Pro	NR	3.22	13.25	P	NR
X	117758578	G	C	*DOCK11*	NM_144658.3:c.3548G>C	p.Gly1183Ala	0.00001	5.53	6.79	D	rs370985549
UW336 Family											
Chr	**bp (hg19)**	**ref**	**alt**	**gene**	**cDNA change**	**AA change**	**ExAC MAF**	**GERP**	**CADD**	**MT**	**rs**
2	3391754	C	CC	*TRAPPC12*	NM_016030.5:c.360_361insC	p.Glu121Argfs*7	NR	1.09	9.89	D	NR
2	3482619	C	T	*TRAPPC12*	NM_016030.5:c.1880C>T	p.Ala627Val	0.000008	5.92	21.3	D	rs768950892
21	37581084	G	A	*DOPEY2*	NM_005128.2:c.563G>A	p.Ser188Asn	0.008263	4.11	20.2	P	rs142091518
21	37597909	C	G	*DOPEY2*	NM_005128.2:c.1417C>G	p.Pro473Ala	0.008141	5.05	17.66	P	rs138343054

alt=alternate base, bp=base pair position (hg19 reference genome), CADD=Combined Annotation Dependent Depletion version 1.0, Chr=Chromosome, D=Disease Causing per Mutation Taster, ExAC MAF=Exome Aggregation Consortium Minor Allele Frequency, GERP=Genomic Evolutionary Rate Profiling, NR=Not Reported, P=Polymorphism per Mutation Taster, ref=reference base, rs= Reference SNP cluster ID